Military Technical College
Kobry El-Kobba
Cairo, Egypt

12-th International Conference
on
Aerospace Sciences &
Aviation Technology

EFFECT OF POLYMER CONCENTRATION ON BEADS FORMATION DURING ELECTRO SPINNING OF NANOFIBERS

El-Leathy* A.M. and Sallam** K.A.

ABSTRACT

An experimental study of beads formation during the electro spinning of nanofibers is reported. Electrostatic charging of a polymer solution (Poly Ethylene Oxide (PEO)) at the tip of a micro needle resulted in the formation of a Taylor cone, from the apex of which a single micro liquid jet is ejected. The jet was then electro spun and the resulting PEO nanofibers with average diameter of 300 nm were deposited on a grounded substrate. The collected nanofibers exhibited bead-like structures depending on: the polymer concentration in the electro spun solution, the applied voltage, the injection pressure and the needle-electrode distance. The beads formation has been a problem for almost a century and the current work approaches this problem form the fluid mechanics point of view. The micro jet near the nozzle exit was observed in-flight using digital holographic microscopy and the collected nanofibers were examined using Scanning Electron Microscopy (SEM). The initial fiber jet diameter, d_o, wave length of jet instability, λ, and the distance along the jet from the needle tip, x, are measured and reported. The results show a strong relationship between the initial jet instability (near the injector exit) and the bead formation on the collected nanofibers.

KEY WORDS

Nanofibers, Electro spinning, Beads and Polymer.

*Assistant professor, Dpt. of Mechanical Power Engineering, Helwan University, Egypt. Currently visiting assistant professor at Oklahoma State University, Oklahoma, USA.

**Assistant professor, Dpt. of Mechanical and Aerospace Engineering, Oklahoma State University, Oklahoma, USA. Corresponding Author: khaled.sallam@okstate.edu.

I. INTRODUCTION

Electro spinning is a process by which polymer nanofibers can be produced using an electrostatically driven jet of polymer solution (or polymer melt). The electric field is generated by applying a high voltage between the metal needle and the collector electrode. The jet then thins away from the needle and subsequently bends and whips. Although there are many papers on electro spinning of nanofibers [1-10, 13-19], the problem of bead formation is still unresolved. There are many factors that affected the formation of beads on nanofibers. These include: the viscosity of the solution, the charge density of the jet, the surface tension of the solution, and the distance from the needle to the grounded collector as well as the ambient air conditions. Fong et. al. [2] found that the surface tension and viscoelastic properties of the PEO polymer solution are the key parameters in the process of bead formation. Jaeger et. al. [9-10] found that the PEO fiber diameter is the main factor that affects bead diameter and spacing as follows: the thinner the fiber, the shorter the distance between the beads and the smaller its diameter. Unfortunately, for each new material being synthesized, the problem of beads formation is still being tackled using time-consuming method of trial-and-error by varying the parameters of the electro spinning process until the beads exist no more. The instability of the polymer jet has a big rule on the fiber bead formation. The literature cites three types of instabilities during the electro spinning process: (1) the axisymetric Rayleigh instability, (2) the electric field-induced axisymetric instability, and (3) the whipping instability [5-6, 14-15, 19]. The objective of the present investigation was to understand the mechanism for beads formation during electro spinning of nanofibers by examining the the effect of initial jet instability (near the injector) on the process of bead-formation. The long term goal of the study is to use phenomenological analyses to construct a universal breakup regime map that characterizes the formation of beads for various test conditions of the electro spinning process and wide variety of polymeric solutions. This new map will accelerate the synthesis of new nanofibers by reducing the cost and effort required to eliminate the beads formation. The instrumentations of the present study include Scanning Electron Microscopy (SEM) to investigate the morphology of the generated nanostructures and digital in-line holography to examine the instabilities along the surface of the PEO polymer solution micro jet near the injector exit.

II. EXPERIMENTAL METHODS

PEO, with an average molecular weight of 9 $x10^5$ g/mol (Scientific Polymer Products Inc.) and distilled water (solvent) were used to prepare the polymer solution. The solutions were prepared at room temperature, and gently stirred to accelerate dissolution and to obtain homogeneous solutions. Two sets of PEO solutions were used in this study: 2 g and 4 g of PEO were dissolved in 100 g of distilled water to form (1.96%) and (3.85%) solutions, respectively. The preparation and characterization of these solutions are summarized in Table 1. The PEO solution was held in a metallic container, which is connected to a needle with an internal diameter of 0.56 mm. The air pressure above the solution was regulated with an air pump such that a drop of the PEO

solution was suspended from the needle tip. The needle was connected to a high-voltage supply (Glassman High Voltage Inc.), which is capable of generating positive DC voltages up to 50 kV. A flat metal plate, placed 19 cm below the needle, was used as a grounded electrode to collect the electro spun nanofibers. When voltage difference was applied between the needle tip and the grounded electrode, the suspended drop at the needle tip was deformed into a conical shape, called the "Taylor cone" [16]. The surface of the drop became unstable, and a jet was ejected from the cone towards the grounded plate. In-line digital holography [11-12] was chosen to study the formation of jet instability because of its ability to capture a three dimensional image with high magnification. The experimental setup is relatively simple only requiring a collimated laser beam and CCD sensor. The optical setup used one beam that was expanded with a 5x objective lens, and then passed directly through the test section to a Cooke Corporation cooled interline transfer CCD camera (Cooke, Model: PCO 2000) having 2048 × 2048 pixels that were 7.4 μm wide by 7.4 μm tall. After the hologram is recorded, it is reconstructed as shown in Figs. 1 and 2. The morphology of the electro spun nanofibers was observed with a Scanning Electron Microscope (JEOL JXM 6400). The nanofibers were collected on microscope slides for SEM measurements.

III. RESULTS AND DISCUSSION

Two PEO solutions were prepared for the present study. The PEO concentration was as follows: (1) 2 g of PEO with distilled water which resulted in beaded fibers, and (2) 4 g of PEO with distilled water which resulted in non-beaded fiber. The instability in electro spinning near the needle tip has limited studies and occurs very rapidly, which requires the use of high-speed photographic techniques. Current work investigated this instability using the measuring techniques that mentioned before. Figs. 1 and 2 show SEM images of the beaded and non-beaded fibers. For the beaded fiber (Fig. 1), the average bead length along the fiber axis is 2 μm; the average bead width perpendicular to the fiber axis is 600 nm, the average fiber diameter of 150 nm. While for the non-beaded fiber (Fig. 2), the average fiber diameter is 280 nm. The fiber diameter for the beaded fiber is less than that of the non-beaded one which is attributed to the extraction of the fiber to form beads. Surface tension is an important parameter in beads formation. It attempts to reduce the surface area per unit mass which attributes to change the jets into spherical shape. On the other hand, there is viscoelastic force which resists the fast change in shape. These two forces explain why beaded fiber (Fig. 1) is less likely to be formed for the more viscous solution, in which increasing the viscosity favors the formation of smooth fibers. Figs. 3 and 4 show reconstructed hologram images using in-line digital holography for the two PEO solutions. From these images it can be seen that the shape of the initial jet, stretched from a Taylor cone into wave-like shape. From these images the instability, λ / d_o, for the two solutions were plotted (Figs. 5 and 6) against the distance from the needle tip, x/d_o, where, d_o, represents the initial fiber diameter. Beyond the Taylor cone, the jet thins slowly and the axis symmetric instabilities for the two PEO solution increase with increasing the distance from the needle tip while for the 2 g beaded fiber the axis symmetric instabilities are greater than the 4 g non-beaded one, in

which beaded fibers were produced while for solution 2 electro spinning has yield smooth fibers. The diameter of the jet as a function of axial distance from the needle tip was measured. Figs. 7 and 8 show the scaling of the jet diameter, d/d_o, as a function of the axial distance, x/d_o, for the two PEO solutions. As the distance, x, increases, the average fiber diameter decreases. These figures also show that increasing the solution viscosity (4g PEO) causes a more rapid initial jet thinning.

V. CONCLUSIONS

Two PEO solutions in distilled water of (1.96%) and (3.85%) were electro spun to produce beaded and non-beaded nanofibers, respectively. The conclusions of the present study were as follows:

- Instability analysis of an electrically driven jet reveals that the solution viscosity has great effects on the formation of beaded fibers, where higher viscosity favors formation of non-beaded fibers.
- The large diameter reduction during the electro spinning process is achieved by stretching and acceleration of a fiber jet as observed in the near-injector region (prior to solidification on the collector plate).
- The results show a strong relationship between the initial jet instability (near the injector exit) and the bead formation on the collected nanofibers.

ACKNOWLEDGMENTS

The support of the first author (A.M. El-Leathy) by the Egyptian Ministry of Higher Education "ParOwn Program" is gratefully acknowledged. The help from Mr. V. Joseph, Mr. J. Lee, and Mr. A. Osta during the initial stage of this research is acknowledged. Initial development of experimental methods was carried out under the National Science Foundation, Grant No. EPS-0132534 Oklahoma-EPSCOR (Nano-Net).

REFERENCES

[1] Colman, P., and Joo, Y., ”Electrospinning of Viscoelastic Boger Fluids: Modeling and Experiments”, Physics of Fluids, Vol. 18, pp. 053102-053114 (2006).

[2] Fong, H., Chun, I., and Reneker, D.H., “Beaded nanofibers formed during electrospinning”, Polymer Journal, Vol. 40, pp. 4585–4592 (1999).

[3] Frenot, A., Chronakis, I., “ Polymer Nanofibers Assembled by Electrospinning”, Current Opinion in Colloid and Interface Science, Vol. 8, pp. 64–75 (2003).

[4] He, J., Wu, Y., Zuo, W., “Critical Length of Straight Jet in Electrospinning”, Polymer, Vol. 46 pp. 12637–12640 (2005).

[5] Hohman, M.M., Shin, Y. M., Rutledge, G.C., and Brenner, M.P., "Electrospinning and Electrically Forced Jets .I. Stability Theory," Physics of Fluids Journal, Vol. 13, pp. 2201- 2220 (2001).

[6] Hohman, M.M., Shin, Y. M., Rutledge, G.C., and Brenner, M.P., "Electrospinning and Electrically Forced Jets. II. Application ," Physics of Fluids Journal, Vol. 13, pp. 2221- 2236 (2001).

[7] Huang, Z., Zhang, Y., Ramakrishna, S., Lim, C., "Electrospinning and Mechanical Characterization of Gelatin Nanofibers", Polymer, Vol. 45 , pp. 5361–5368 (2004).

[8] Jaeger, R., Bergshoef, M., Batlle, C., Schonherr, H., and Vancso, J., "Electrospinning of ultra-thin polymer fibers", Macromolecular Symposium, Vol. 127, pp. 141-150 (1998).

[9] Jaeger, R., Scho1nherr, H., and Vancso, G. J., "Chain Packing in Electro-Spun Poly(ethylene oxide) Visualized by Atomic Force Microscopy", Macromolecules, Vol. 29, pp. 7634-7636 (1996).

[10] Kenawy, E., Layman, J., Watkins, J., Bowlin, G., Matthews, J., Simpson, D., Wnek, G., "Electrospinning of Poly (Ethylene-co-Vinyl Alcohol) Fibers', Biomaterials, Vol. 24, pp. 907–913 (2003).

[11] Kreis, T.M., Adams, M. and Jüptner, W.P., "Methods of Digital Holography: A Comparison", SPIE, Vol. 3098, pp. 224-233 (1997).

[12] Miller, B., Sallam, K.A., Lin, K.-C. and Carter, C., "Digital Holographic Spray Analyzer", ASME Joint U.S.-European Fluids Engineering Summer Meeting, FEDSM2006-98526 (2006).

[13] Samatham, R., Kim, K., "Electric Current as a Control Variable in the Electrospinning Process", Polymer Engineering and Science, Vol. 46, No.7, pp. 954-959 (2006).

[14] Shin, Y. M., Hohman, M.M., Brenner, M.P., and Rutledge, G.C., "Electrospinning: A Wipping Fluid Jet Generates Submicron Polymer Fibers," Applied Physics letters Journal, Vol. 78, pp. 1149-1151 (2001).

[15] Shin, Y. M., Hohman, M.M., Brenner, M.P., and Rutledge, G.C., "Experimental Characterization of Electrospinning: The Electrically Forced Jet and Instabilities," Polymer Journal, Vol. 42, pp. 9955-9967 (2001).

[16] Taylor, G. I., "Disintegration of water drops in an electric field", Proceedings of the Royal Society of London, Series A, Mathematical and Physical Sciences, Vol. 280, No. 1382, pp 383-397 (1964).

[17] Theron, S., Yarin, A., Zussman, E., Kroll, E., "Multiple Jets in Electrospinning: Experiment and Modeling", Polymer, Vol. 46 , pp. 2889–2899 (2005).

[18] Wang, M., Singh, H., Hatton, T., Rutledge, G., "Field-Responsive Superparamagnetic Composite Nanofibers by Electrospinning', Polymer, Vol. 45, pp. 5505–5514 (2004).

[19] Zuo, W., Zhu, M., Yang, W., Yu, H., Chen, Y., and Zhang, Y., "Experimental Study on Relationship between Jet Instability and Formation of Beaded Fibers during Electrospining", Polymer Engineering and Science, Vol. 45, No. 5 pp. 704-709 (2005).

Table 1. Summary of the test condition.

Test Condition	PEO (g)	Water (g)	Applied voltage (kV)	Flying distance (cm)	RH%	T °C
1	2	100	20	19	25	24
2	4	100	20	19	24	25

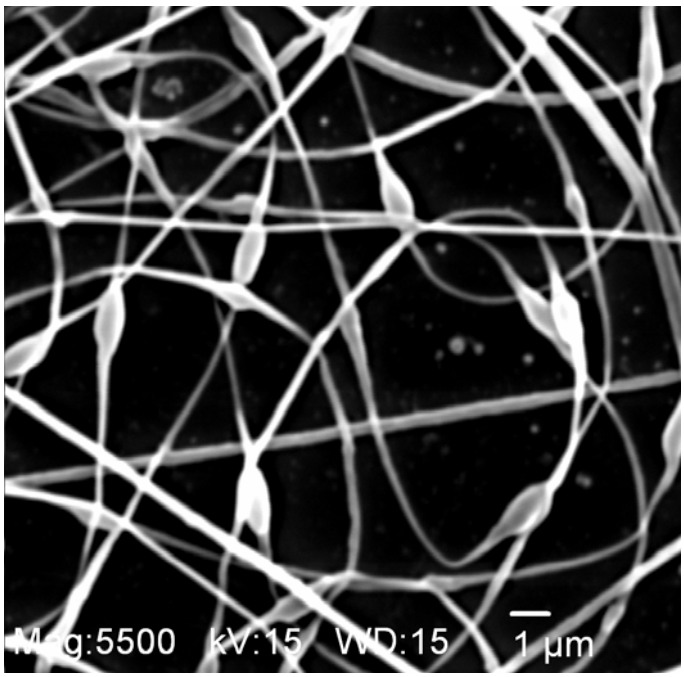

Fig. 1. The beaded nanofibers (2g PEO).

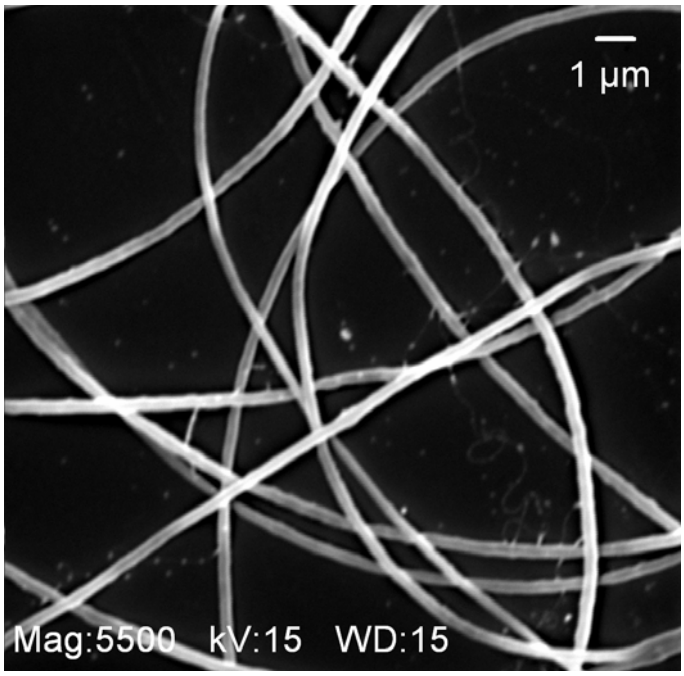

Fig. 2. The non-beaded nanofibers (4g PEO).

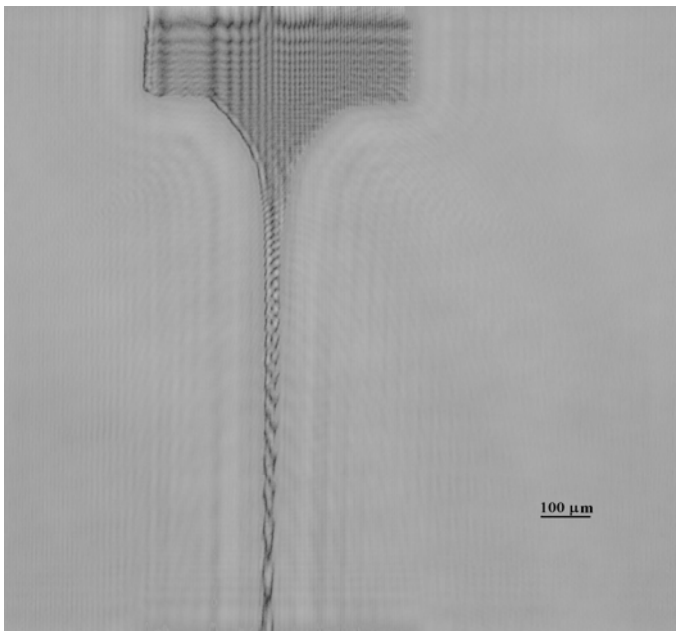

Fig. 3. Reconstructed hologram of the micro jet associated with the beaded nanofiber (2g PEO).

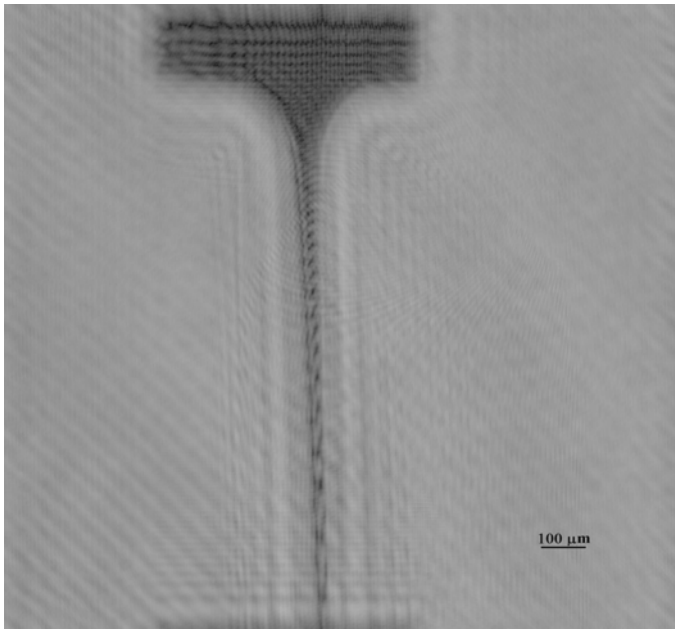

Fig. 4. Reconstructed hologram of the micro jet associated with non-beaded nanofiber (4g PEO).

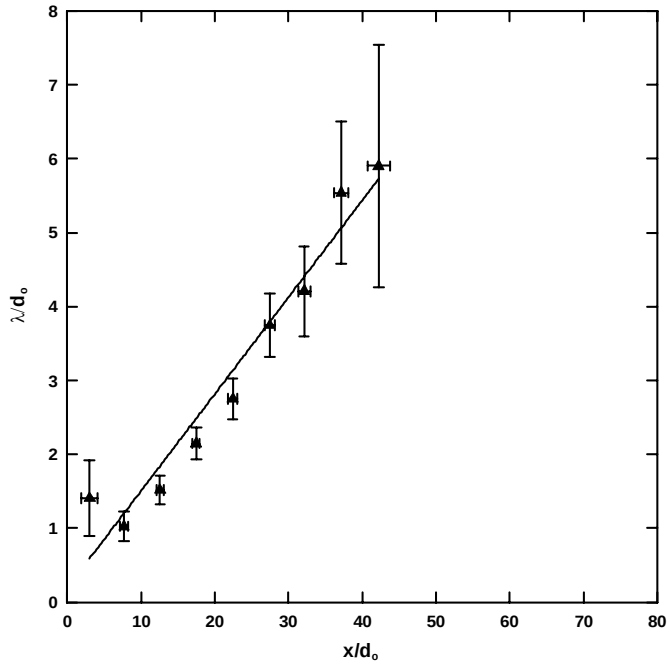

Fig. 5. Normalized wavelength of the instabilities along the liquid jet vs. the normalized distance from the needle tip for the beaded fiber (2g PEO).

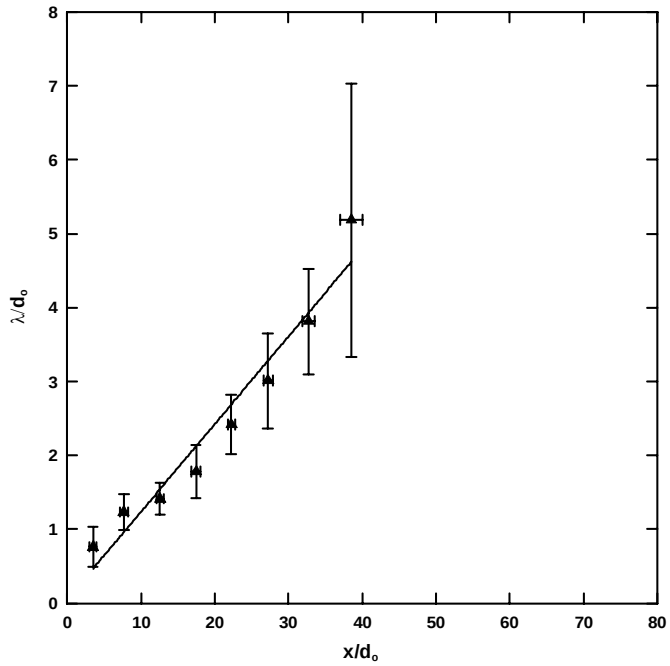

Fig. 6. Normalized wavelength of the instabilities along the liquid jet v. the normalized distance from the needle tip for the non-beaded fiber (4g PEO).

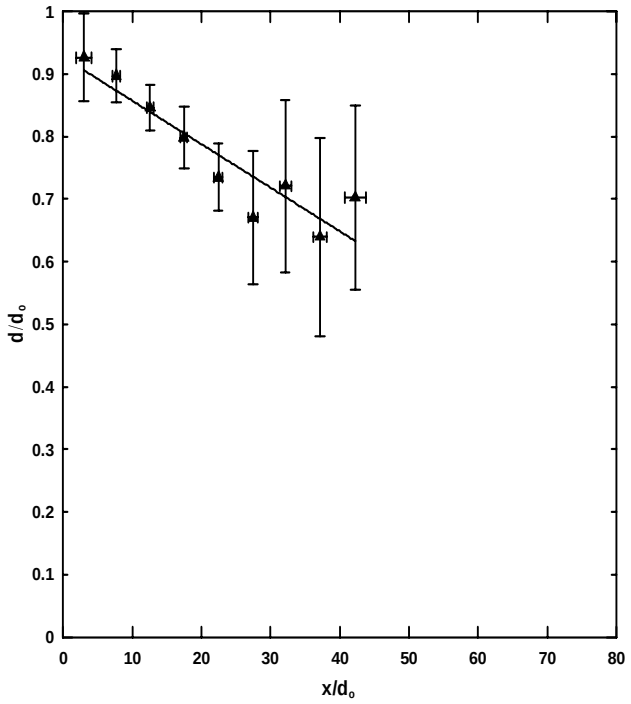

Fig. 7. Normalized jet diameter vs. the normalized distance from the needle tip for the beaded fiber (2g PEO).

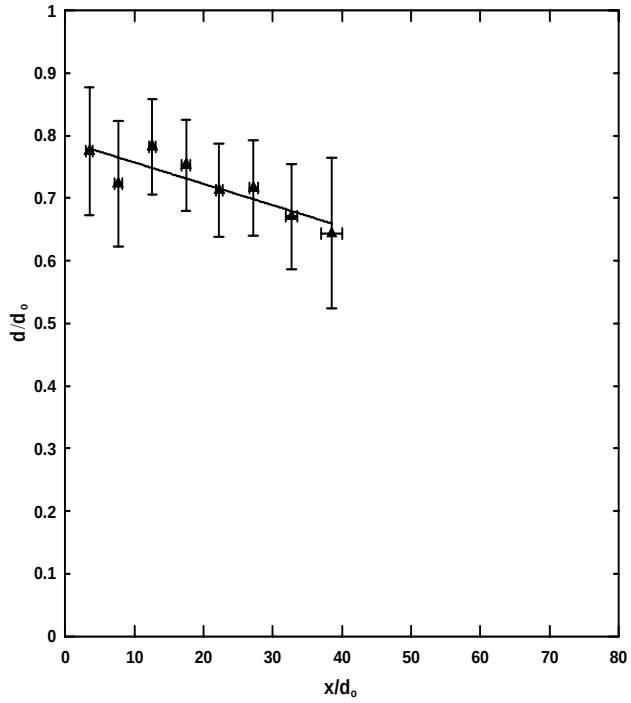

Fig. 8. Normalized jet diameter vs. the normalized distance from the needle tip for the non-beaded fiber (4g PEO).